Available online at www.sciencedirect.com

SciVerse ScienceDirect

Ceramics International 38 (2012) 4325–4329

CERAMICS INTERNATIONAL

www.elsevier.com/locate/ceramint

# Fabricated and improved electrochemical properties of $Li_2MnSiO_4$ cathodes by hydrothermal reaction for Li-ion batteries

Shaohua Luo [a,*], Ming Wang [a,b], Weina Sun [a]

[a] Department of Materials Science and Engineering, Northeastern University at Qinhuangdao Branch, Qinhuangdao, Hebei 066004, China
[b] Shanghai Institute of Ceramics, Chinese Academy of Sciences, Shanghai 200050, China

Received 19 November 2011; received in revised form 4 February 2012; accepted 7 February 2012
Available online 15 February 2012

**Abstract**

$Li_2MnSiO_4$ cathode materials were hydrothermally synthesized from commercial LiOH, $Mn(Ac)_2$, $Si(OC_2H_5)_4$ in aqueous solution. The technic factors, such as temperature, time, compactness and molar ratio of Li:Mn:Si, were systematically studied by orthogonal test method. The optimization hydrothermal synthesis of $Li_2MnSiO_4$ is determined as the condition of the reaction temperature at 200 °C, the reaction time of 72 h, the compactness of 75 vol% and the molar ratio of Li:Mn:Si as 2:1:1. Among them, the influence of the temperature on the electrochemical performance of the sample is the greatest. An X-ray diffraction pattern confirms the formation of the orthorhombic structure with $Pmn2_1$ space group. The Li/$Li_2MnSiO_4$ cells delivered an initial discharge capacity of 226 mAh/g for as-synthesized following heat-treated $Li_2MnSiO_4$ under the optimized conditions. It is surprising to note that heat-treated $Li_2MnSiO_4$ exhibits more stable and superior cycling performance than reported values elsewhere, which is due to the unique morphology as well as well crystallization during high temperature sintering.


*Keywords:* $Li_2MnSiO_4$; Cathode materials; Hydrothermal reaction; Orthogonal test

## 1. Introduction

More recently, lithium transition-metal orthosilicates $Li_2MSiO_4$ (M = Fe, Mn, Co, Ni) are rapidly attracting much attention as a candidate for cathode material due to availability of abundant elements and possibility of multi-electron reaction [1]. Among them, $Li_2MnSiO_4$ is a potentially promising candidate for the high theoretical capacity (333 mAh/g) and high operating voltage [2]. However, it shows poor electrochemical performance and capacity retention. In order to solve these problems, many efforts have been paid through several groups, including carbon coating, Mn-site solid-solution doping by Fe and solution route to avoiding second phases [3–6]. Till now, the structural properties of $Li_2MnSiO_4$ are unclear and it depends on the synthesis conditions and starting materials used. Several authors claimed the existence of three kinds of polymorphs for $Li_2MnSiO_4$ which comprises $Pmn2_1$, $Pmnb$ and $P2_1/n$ space groups, respectively [7]. For example, Dominko et al. [8,9] reported $Li_2MnSiO_4$ having $Pmnb$ space group at 900 °C (all the synthesis routes, solid-state, sol–gel, hydrothermal, etc.), Politaev et al. [10] reported the existence of the $P2_1/n$ space group by solid-state reactions at 750–1150 °C, and Belharouak et al. [11] also claimed the existence of the $Pmn2_1$ space group at 800 °C by the sol–gel route. The different structures of $Li_2MnSiO_4$ materials by different synthesis methods further effect lithium intercalation behavior.

Moreover, pure $Li_2MnSiO_4$ can seldom obtained by ordinary synthesis methods [2,5,6]. Hydrothermal synthesis is one of the routes to prepare pure phase, small and homogeneous particle size materials with desired morphology at relatively lower temperature than that in solid state techniques. However, it is rather difficult to determine the suitable conditions. In this paper, we systematically studied the technic factors of hydrothermal reaction and successfully prepared pure phase $Li_2MnSiO_4$ using hydrothermal reaction and then annealing at 700 °C.

## 2. Experimental

The starting materials for the hydrothermal reaction were $LiOH{\cdot}H_2O$, $Mn(Ac)_2{\cdot}4H_2O$ and $Si(OC_2H_5)_4$. The concentration

* Corresponding author. Tel.: +86 335 8047760.
*E-mail address:* luosh00@126.com (S. Luo).

0272-8842/$36.00 
doi:10.1016/j.ceramint.2012.02.014

of $Mn(Ac)_2{\cdot}4H_2O$ and $Si(OC_2H_5)_4$ was controlled to be 0.015 mol. A mixture in a designed molar ratio of the raw materials was ball-milled for 10 min in de-ionized water. The slurry was transferred to a 110 ml Teflon-lined vessel sealed in a stainless steel autoclave and heated at 150–200 °C for several days. After cooling to room temperature, precipitates were collected by suction filtration and then parched for the vacuum drying. The dried precipitates were further annealed at 700 °C for 10 h in nitrogen atmosphere.

The phase identification of the products was confirmed by a powder X-ray diffractometer (DX-2500, Fangyuan, China). Particle morphology of the products was observed with a scanning electron microscope (FE-SEM, S-4800-II, Hitachi, Japan). The IR spectra were measured on Shimadzu FIR-8400, Japan. The electrode was composed of the sample, acetylene black and PVDF in a weight ratio of 75:17:8. These electrodes were dried under vacuum at 120 °C for at least 8 h before the 2032 coin cells assembly inside an argon-filled glove box. Cells were cycled galvanostatically with several times for the charge–discharge testing using LAND CT 2001A system between 1.5 and 4.8 V vs. Li at room temperature.

## 3. Results and discussion

### 3.1. Orthogonal test

In order to optimize the synthetic conditions and study their effects on the electrochemical performance of sample, a $L_9$ ($3^4$) orthogonal experiment was performed. A $L_9$ ($3^4$) matrix, which is an orthogonal array of four factors and three levels, was employed to assign the considered factors and levels. Nine trials were carried out according to the $L_9$ ($3^4$) matrix to complete the optimization process [12,13]. The factors and levels were shown in Table 1, which shows 150 °C, 175 °C, and 200 °C for hydrothermal reaction temperature, 24 h, 48 h, and 72 h for hydrothermal reaction time, 67 vol%, 75 vol%, and 83 vol% for compactness and the molar ratio of Li:Mn:Si as 2:1:1, 3:1:1, and 4:1:1.

From Fig. 1, as to factor A, if the reaction temperature reaches level 3 (200 °C), the initial discharge capability will own the maximum value. So $A_3$ is the best choice. As to factor B, since it has a minimum significance, the influence of the reaction time on synthesizing $Li_2MnSiO_4$ is least. Considering the result of the crystallinity experiment, $B_3$ is adopted. As to factor C, if the compactness exceeds level 2 (75 vol%), the initial discharge capability will not increase. So $C_2$ is chosen.

Table 1
Factors and levels for orthogonal test.

| Level | Factors | | | |
|---|---|---|---|---|
| | A Reaction temperature/°C | B Reaction time/h | C Compactness/% | D Li:Mn:Si |
| 1 | 150 | 24 | 67 | 2:1:1 |
| 2 | 175 | 48 | 75 | 3:1:1 |
| 3 | 200 | 72 | 83 | 4:1:1 |

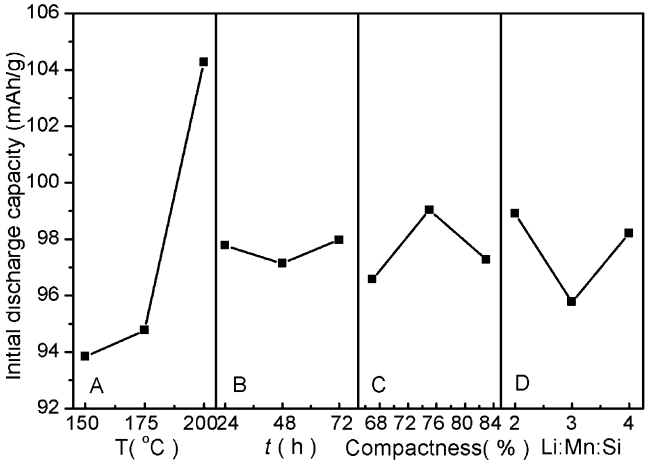


Fig. 1. Relationships between factors and capacity in orthogonal test.

As to factor D, if the molar ratio for Li:Mn:Si is 2:1:1, the result will be better. So $D_1$ is the best choice. Considering the crystallinity and cycling behavior, the optimization for synthesis of cathode material $Li_2MnSiO_4$ is $A_3B_3C_2D_1$.

Fig. 2 represents XRD pattern of $Li_2MnSiO_4$ prepared in hydrothermal orthogonal test. The majority of reflectance peaks can be assigned to $Li_2MnSiO_4$ phase, which have an orthorhombic unit cell in space group $Pmn2_1$. However, a impurity $Li_2SiO_3$ are detected in several samples, which are marked with an asterisk in Fig. 2. The molar ratio of Li:Mn:Si shows great influence on the content of impurity and crystallization. S1, S5 and S9 with a molar ratio of Li:Mn:Si as 2:1:1 have imperfect crystal with obvious large wide peak of XRD. With increase of the molar ratio of Li:Mn:Si, the sample XRD peaks of main phase $Li_2MnSiO_4$ are sharp, but the intensity of impure phase $Li_2SiO_3$ are increasing. The other factors reaction temperature and reaction time show little influence on the degree of crystallization and impure phase.

### 3.2. Confirmation test

The molar ratio for $LiOH{\cdot}H_2O$:$Mn(Ac)_2{\cdot}4H_2O$:$Si(OC_2H_5)_4$ was 2:1:1. The raw materials were ball-milled in 82.5 ml de-ionized water for 10 min. The mixed solution was put into a 110 ml reactor, and it was heated at 200 °C for 72 h. After the hydrothermal process, the precipitated powder was filtered to separate, washed and dried. The sample was further annealed at 700 °C for 10 h in nitrogen atmosphere. The as-prepared sample in optimized hydrothermal process and the annealed one are denoted as HT-LMS and A-LMS, respectively.

Fig. 3 shows XRD patterns of HT-LMS and the A-LMS in confirmation test. HT-LMS ones were broad, suggesting a low degree of crystallinity. Both patterns agree well with that of the orthorhombic structure and little impure phase could be detected. Almost all Bragg peaks can be indexed to the orthorhombic unit cell in space group $Pmn2_1$. The phase analysis results indicate that all diffraction peaks can be assigned to the $Li_2MnSiO_4$ phase. Five intense diffraction peaks of A-LMS are corresponding to the (1 1 0), (0 1 1), (1 1 1), (2 1 0) and (0 0 2) planes, respectively. No impure phases were

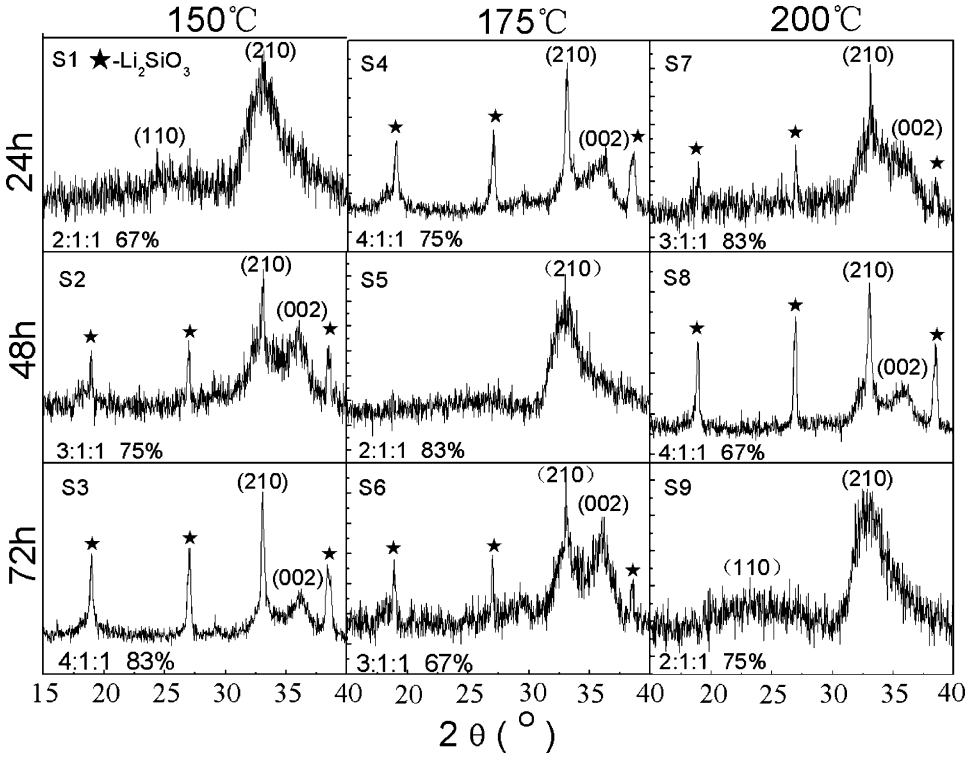


Fig. 2. X-ray diffraction pattern of $Li_2MnSiO_4$ prepared in hydrothermal orthogonal test.

detected in the XRD pattern. The lattice constants have been calculated to be $a = 0.63075$ nm, $b = 0.53584$ nm, and $c = 0.50484$ nm. These values are consistent with those reported previously [2,4]. Fig. 4 presents the FTIR spectrum of the two samples in the range of 400–1200 $cm^{-1}$. As is known, the bonds in IR spectra of inorganic compounds always appear below 1500 $cm^{-1}$. In Fig. 4, the positions of 890 $cm^{-1}$, 926 $cm^{-1}$, 578 $cm^{-1}$ and 530 $cm^{-1}$ are characteristic absorption peaks of [$SiO_4$]. 890 $cm^{-1}$ and 926 $cm^{-1}$ peaks exhibit $\nu_1$ and $\nu_3$ mode of Si–O bonds, while 530 $cm^{-1}$ and 578 $cm^{-1}$ is assigned to $\nu_4$ vibrations [14]. 426 $cm^{-1}$ and 485 $cm^{-1}$ low-frequency bonds perhaps indicate lithium ion motion [15]. The adsorption band around 735 $cm^{-1}$ is perhaps attributed to the bending vibration of Si–O–Si bonds in some [$SiO_3$] group due to reducible reaction condition. After being annealed, the peaks of samples become sharper, which also indicates that annealed LMS samples are well crystallized.

Fig. 5 represents the morphological features of HT-LMS and A-LMS. The 20 nm thin of flower-like morphology overlap together is formed during the nucleation growth in the presence of water under optimized hydrothermal treatment in Fig. 5a. The A-LMS flake shows larger and thicker than the HT-LMS. It appeared as highly crystallized along with flake margin of the flower petals and existed some tiny spherical crystals bounded between the flower petals. As expected, such morphology may translate into good electrochemical properties due to its high surface area, unique morphology and high interconnection with

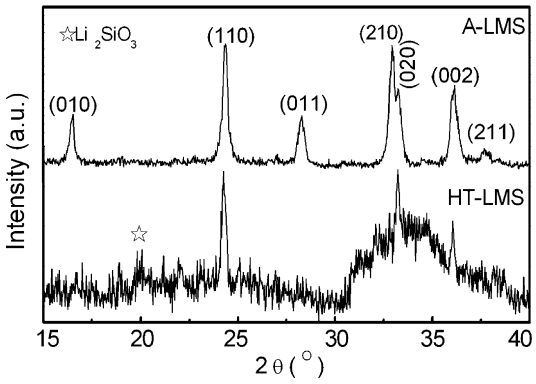


Fig. 3. XRD patterns of $Li_2MnSiO_4$ as-prepared under hydrothermal optimized conditions (HT-LMS) and annealed at 700 °C (A-LMS).

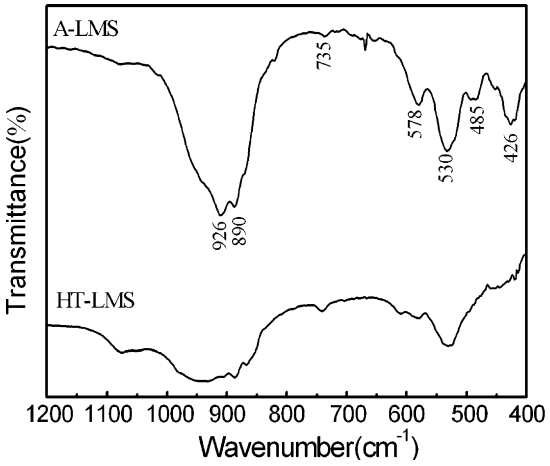


Fig. 4. FTIR spectrum of $Li_2MnSiO_4$ as-prepared under hydrothermal optimized conditions (HT-LMS) and annealed at 700 °C (A-LMS).

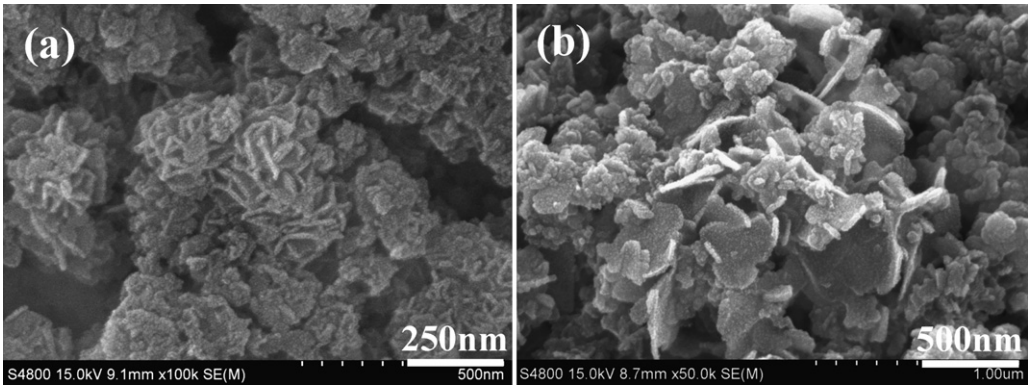


Fig. 5. SEM images of $Li_2MnSiO_4$ samples: (a) as-prepared sample by hydrothermal optimized conditions (HT-LMS) and (b) annealed sample at 700 °C (A-LMS).

nearest neighboring particles rather than the conventional particles for diffusion of $Li^+$ ions.

The cell performance of heat-treated $Li_2MnSiO_4$ materials (A-LMS) and HT-LMS at *C*/20 rate against lithium is shown in Fig. 6. The optimized sample shows superior specific charge–discharge capacity and cycling performance compared with the ones of nine samples of orthogonal test as shown in Fig. 1. The initial charge and discharge capacity of A-LMS is 300 mAh/g and 226 mAh/g, respectively, which is higher than that of HT-LMS (193 mAh/g and 125 mAh/g). The cycling profiles of the Li/A-LMS are very stable (∼130 mAh/g) after the 10 cycles when compared with the HT-LMS material with columbic efficiency over 94%. At the same time, HT-LMS experiencing the continuous capacity fade even after 40 cycles presented a lower discharge capacity profile (68 mAh/g). Generally, excellent cycling performance and stable electrochemical stability of A-LMS may be ascribed to the thin flat shape of the crystal morphology, which has a profound effect on the formulation of the high-speed process with sufficient contact with other cell components (binder and towards current collector). In addition, the crystallization of such particles cannot be excluded during high temperature sintering.

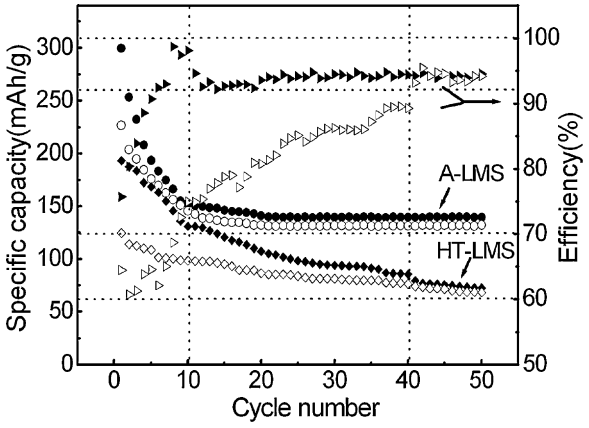


Fig. 6. Charge and discharge capacity cycling performance of A-LMS and HT-LMS electrodes at *C*/20 rate, and the charge/discharge efficiency (solid and hollow trigon).

## 4. Conclusions

To conclude, the hydrothermal route under optimized technical parameters was employed for the successful preparation of $Li_2MnSiO_4$ materials with flower-like morphology from raw materials of LiOH, $Mn(Ac)_2$ and $Si(OC_2H_5)_4$. X-ray reflections of heat-treated sample confirmed the only $Li_2MnSiO_4$ phase without less amount of $Li_2SiO_3$. The heat-treated $Li_2MnSiO_4$ exhibited superior performance in terms of its electrochemical stability of ∼125 mAh/g and it was achieved by well-crystallization as well as morphology and pure phase.

## Acknowledgments

This work was supported by the Fundamental Research Funds for the Central Universities (No. N100423002), Priority Research item in Application Foundation Research Plan of Hebei (No. 09963910D), Natural Science Research Guiding Project of Hebei Education Department (No. Z2008408), and Ningxia National Science Foundation (No. NZ0843).

## References

[1] A. Nytén, A. Abouimrane, M. Armand, T. Gustafsson, J.O. Thomas, Electrochemical performance of $Li_2FeSiO_4$ as a new Li-battery cathode material, Electrochem. Commun. 7 (2005) 156–160.

[2] R. Dominko, M. Bele, M. Gaberscek, A. Meden, M. Remskar, J. Jamnik, Structure and electrochemical performance of $Li_2MnSiO_4$ and $Li_2FeSiO_4$ as potential Li-battery cathode materials, Electrochem. Commun. 8 (2006) 217–222.

[3] Z.L. Gong, Y.X. Li, Y. Yang, Synthesis and characterization of $Li_2Mn_xFe_{1-x}SiO_4$ as a cathode material for lithium-ion batteries, Electrochem. Solid-State Lett. 9 (12) (2006) A542–A544.

[4] Y.X. Li, Z.L. Gong, Y. Yang, Synthesis and characterization of $Li_2MnSiO_4$/C nanocomposite cathode material for lithium ion batteries, J. Power Sources 174 (2007) 528–532.

[5] P. Ghosh, S. Mahanty, R.N. Basu, Improved electrochemical performance of $Li_2MnSiO_4$/C composite synthesized by combustion technique, J. Electrochem. Soc. 156 (8) (2009) A677–A681.

[6] W.G. Liu, Y.H. Xu, R. Yang, Synthesis, characterization and electrochemical performance of $Li_2MnSiO_4$/C cathode material by solid-state reaction, J. Alloys Compd. 480 (2009) L1–L4.

[7] A. Boulineau, C. Sirisopanaporn, R. Dominko, A.R. Armstrong, P.G. Brucec, C. Masquelier, Polymorphism and structural defects in $Li_2FeSiO_4$, Dalton Trans. 39 (2010) 6310–6316.
[8] R. Dominko, C. Sirisopanaporn, A. Boulineau, C. Masquelier, C. Hanzel, I. Arčon, A. Kodre, G. Mali, M. Gaberscek, Lithium Battery Discussion on Electrode Materials, Arcachon, France, September 20–25, 2009, 2009.
[9] M.E.A. Arroyo-de Dompablo, R. Dominko, J.M.G. Amores, L. Dupont, G. Mali, H. Ehrenberg, J. Jamnik, E. Moran, On the energetic stability and electrochemistry of $Li_2MnSiO_4$ polymorphs, Chem. Mater. 20 (2008) 5574–5584.
[10] V.V. Politaev, A.A. Petrenko, V.B. Nalbandyan, B.S. Medvedev, E.S. Shvetsova, Crystal structure, phase relations and electrochemical properties of monoclinic $Li_2MnSiO_4$, J. Solid State Chem. 180 (2007) 1045–1050.
[11] I. Belharouak, A. Abouimrane, K. Amine, Structural and electrochemical characterization of $Li_2MnSiO_4$ cathode material, J. Phys. Chem. C 113 (2009) 20733–20737.
[12] J.Y. Li, S.H. Luo, W.H. Yao, Z.T. Zhang, Role of second phase in (Nb, Ce, Si, Ca)-doped $TiO_2$ varistor ceramics, Mater. Lett. 57 (2003) 3748–3754.
[13] X.G. Gao, G.R. Hu, Z.D. Peng, K. Du, $LiFePO_4$ cathode power with high energy density synthesized by water quenching treatment, Electrochim. Acta 54 (2009) 4777–4782.
[14] K. Zaghib, A.A. Salah, N. Ravet, A. Mauger, F. Gendron, C.M. Julien, Structural, magnetic and electrochemical properties of lithium iron orthosilicate, J. Power Sources 160 (2) (2006) 1381–1386.
[15] C.M. Burba, R. Frech, Raman and FTIR spectroscopic study of $Li_xFePO_4$ ($0 \leq x \leq 1$), J. Electrochem. Soc. 151 (7) (2004) A1032–A1038.